International Journal of Engineering Trends and Technology
ISSN: 2231–5381 / https://doi.org/10.14445/22315381/IJETT-V73I2P123

Volume 73 Issue 2, 259-265, February 2025

Review Article

Recent Advances in the Development of Thin Films for the Solar Cell Applications

Ho Soonmin

Faculty of Health and Life Sciences, INTI International University, Malaysia.

Corresponding Author : soonmin.ho@newinti.edu.my

Received: 06 September 2024 Revised: 07 November 2024 Accepted: 11 December 2024 Published: 21 February 2025

Abstract - *Thin films have been synthesized through vacuum-based deposition methods and chemical deposition techniques. Prepared films could be used for solar cell application due to the appropriate band gap, excellent absorption coefficient value and lower production costs. In this work, photovoltaic parameters will be reported, and several properties such as fill factor, power conversion efficiency, open circuit voltage (V_{oc}) and short circuit current (I_{sc}) will be demonstrated. Experimental findings confirmed that properties behaviors are strongly dependent on the experimental conditions.*

Keywords - *Power conversion efficiency, Photovoltaic, Energy efficiency, Fill factor, Thin films, Energy consumption.*

1. Introduction

An electrical device that can generate power from sunshine is a solar cell. As far as we are aware, first-generation (Table 1) conventional crystalline silicon technology has not been proven as cost-effective as thin film solar cells have [1]. They also offer several other benefits, such as being lighter, more flexible [2], and generating less drag. Second generation photovoltaic cells include this kind of solar cell, and the films' thickness typically ranges from nanometres [3] to micrometres. Many researchers have stated that different deposition processes have been used to generate thin films that are up to date. In general, the films created with the costly vacuum-based deposition process [4] yielded good power conversion efficiency. However, the solution-based deposition approach [5] was used to create absorber materials to reduce the cost of solar cell construction. This study examined and evaluated the manufactured solar cell's power conversion efficiency [6]. The test's definition is the power generated by the constructed solar cell divided by the amount of incident solar energy that enters the cell each time [7].

Table 1. Solar cell technologies

1st generation	2nd generation A	3rd generation
• Monocrystalline silicon • Polycrystalline silicon	• Amorphous silicon • Cadmium sulphide • Copper indium gallium selenide • Cadmium Telluride	• Polymer solar cells • Perovskite solar cells • Dye sensitized solar cells

Short circuit current is a crucial measure that assesses the efficiency of a solar cell in transforming sunlight into electrical energy. Open circuit voltage is the potential difference in electricity between the two terminals of a device when it is not connected to any circuit. The fill factor is an important electrical metric that assesses the efficiency of solar cells. It is the ratio of the highest power a solar cell can generate to the multiplication of its short-circuit current and open circuit voltage. Power conversion efficiency indicates the effectiveness of a device in transforming input power into output power. It is determined by taking the output power, dividing it by the input power, and then multiplying the result by 100. In this work, thin films have been produced using various deposition techniques. The photovoltaic properties of the prepared films have been studied. Fill factor, power conversion efficiency, open circuit voltage and short circuit current were reported.

2. Literature Survey

Generally, several photovoltaic parameters will be studied to investigate the performance of the fabricated solar cells. When no current is delivered [8], the voltage differential between two terminals is known as the open circuit voltage (V_{oc}). The greatest voltage a solar panel can generate under typical test settings is denoted as V_{oc}. These parameters include a 25°C cell temperature, a 1000 W/m^2 light intensity, and a 1.5 atmospheric density. The current that flows when the terminals are compelled to have a zero-voltage differential is the short circuit current (I_{sc}). When a solar panel is linked to a device [9], such as an inverter or charge controller, the maximum current that the panel can manage is determined by its I_{sc} value. One crucial metric you may use to assess the

effectiveness of solar cells is the fill factor [10]. You must divide a cell's maximum potential power output by its actual power output to get the fill factor. This will provide you with a measurement that you may use to evaluate your solar cell's performance. Higher fill factor solar cells are more sought-after since they are more efficient. Series resistance (R_s) and shunt resistance ($R_s$ht) are the factors that affect the fill factor. Series resistance is the internal components of the cell's resistance, whereas shunt resistance is the resistance resulting from external connections. The fill factor measures how well-balanced these two resistances are inside a device; they work in opposition to one another. Any resistance at the external connections, through other device components, or between device layers is referred to as series resistance. Your solar cell's efficiency will decrease because of increased series resistance since it will allow less current to pass through it. Solar cells need to be built with low material resistance and enhanced contact design to de crease series resistance [11].

Cu_2ZnSnS_4 (CZTS)-absorber nanoparticles may be made economically and ecologically benignly by Chinho and colleagues [12] utilizing a mechanochemical approach with ethanol, butanol, and methyl ethyl ketone as solvents. The samples that were deposited had a single phase and kesterite crystal structure. The morphological outcomes showed that annealing improved the surface morphology. Thin film optical bandgaps were p-type and ranged from 1.57 to 1.57 eV. There were reports on the as-deposited thin films with (S0_Na) and without Na (S0) solution. The focus was on thin films that were annealed with Na solution at 500 °C (S1_Na), 520 °C (S2_Na), and 550 °C (S3_Na). Conversely, in that order, the samples annealed without Na at 500 °C, 520 °C, and 550 °C were designated as S1, S2, and S3. The photovoltaic device was combined with CZTS absorber layers, both with and without Na, such as SLG/Mo/ CZTS:Na or CZTS/CdS/i-ZnO/ZnO:Al/Ni-Ag. Every photovoltaic device has an overall active area of 0.40 cm^2. The results show that power conversion efficiency was increased in solar devices when the sodium layer was increased.

This might be because CZTS has better crystallinity, which lowers flaws at grain boundaries. It was noticed that samples S1 and S3_Na showed poor performance, which may have been caused by pinholes. Shunting issues with the device are usually caused by the existence of pinholes. Additionally, the presence of voids might lead to additional flaws and higher internal resistance, which would reduce the PV device's performance. As a result, samples S2 and S3 perform slightly differently, which might be because of the voids created by the uneven grain development. Finally, sample S2_Na showed the highest performance of all the devices, with a V_{oc} of 274 mV, an efficiency of 0.16 %, a I_{sc} of 1.61 $mAcm^{-2}$, and a fill factor of 37.48 % (Table 2). Less power conversion efficiency could be found using a vacuum-based method compared to a CZTS-based photovoltaic system (9.2 % to 11 %) because of small-sized grains, which may result from suboptimal sulfurization and Na incorporation processes. High conversion efficiency is best achieved when the Zn/Sn=1.2 and Cu/(Zn + Sn)=0.8); as a result, the CZTS sample elemental composition has to be optimized. The CZTS samples' mobility, which ranged from 2.201 to 3.559 cm^2/Vs, was in line with that of other thin film reports. On the other hand, researchers have reported that the resistivity rises, and the carrier density falls with increasing annealing temperature. The great mobility and low resistivity of samples S1 and S1-Na might be attributed to their carbon content. The voids and tiny grain sizes might be the cause of this. There is still an opportunity for improvement even if the current figures for resistivity (10^{-3}–9.7 Ω.cm), carrier density (10^{16}–10^{20} cm^{-3}), and mobility (0.1–10 cm^2/V.s) for CZTS samples.

RF sputtering created CdS/CdTe ultrathin devices with varying CdS thin-film thicknesses [13]. Soda-lime glass/SnO_2: F/ZnO substrates were used as the substrate. For manufactured solar devices, the CdS thin-film thickness was 70, 110, and 135 nm, whereas the CdTe thin-film thickness was 620 nm. When the film thickness is 70 nm, the presence of sulfur vacancies will enhance the electrical characteristics by causing carriers to increase. Power conversion efficiency, V_{oc} and I_{sc} were 4.56%, 0.6V, and 16.39 mA/cm2, respectively. On the other hand, the open-circuit voltage (V_{oc}) was observed to be 0.53 V and 0.52 V when film thicknesses were 110 and 135 nm, respectively. Research findings revealed a higher transmittance value (about 28%) for devices with a film thickness of 110 and 70 nm compared to 135 nm (about 21%). It was noted that semi-transparent solar cells may be made from using this technique. Gayan and co-workers [14] analyzed and compared the effects of nitrogen (N_2) purging in the CdS deposition bath and the subsequent N_2 annealing with traditional CdS films deposited without purging and annealed at room temperature. Fluorine-doped tin oxide glass slides were used as the substrate for all films, which were created at a temperature of 80 °C using the chemical bath deposition technique. Throughout the CdS deposition procedure, nitrogen gas was added to the deposition bath to deposit N_2-purged layers. After that, the N_2 purged and unpurged films were either annealed in an ambient air environment or at temperatures between 100 °C and 500 °C for an hour.

Table 2. Photovoltaic behaviors of CZTS films without and with sodium layer. [12]

Sample Name	I_{sc} (mA/ cm^2)	V_{oc} (mV)	Power Conversion Efficiency (%)	Fill factor (%)
SC-S1	0.48	280	0.05	38.64
SC-S2	0.85	275	0.09	41.42
SC-S3	0.74	320	0.1	44.25
SC-S1-Na	1.47	201	0.1	35.16
SC-S2-Na	1.61	274	0.16	37.48
SC-S3-Na	1.33	198	0.09	34.13

The variance in the photoelectrochemical cell's open circuit voltage in relation to the annealing temperature for each film in photoelectrochemical research. Based on the results, 300 °C appears to have created the films with the maximum V_{OC}, regardless of the annealing method used. In addition, out of all the films, film N_2-CdS/N_2 had the maximum V_{OC} at an annealing temperature of 300 °C. The photoelectrochemical cell's short circuit current fluctuates depending on the annealing temperature for each film. All the films exhibit an initial rise in I_{SC} before it begins to decline around 300 °C, which is consistent with V_{OC} behavior.

Additionally, it is evident that N_2-CdS/N_2 has greater I_{SC} values than the other four films at all annealing temperatures, with the maximum I_{SC} value being measured at 300 °C. It is well known that annealing increases a material's crystallinity by facilitating the move of atoms into a stable location using thermal energy. Thus, regardless of the annealing and deposition techniques, an increase in the annealing temperature should lead to an improvement in the crystallinity of the CdS films. It is reasonable to justify the films' improved electrical characteristics up to a 300 °C annealing temperature. Sulfur (S) may, however, escape the CdS films at annealing temperatures higher than 375 °C. CdS films that are not stoichiometric may retain this effect. Electrical characteristics drop because of small grain size, decreased crystallinity, and the presence of defects, including surface flaws, structural dislocations, and disorders. The low degree of crystallinity that may be introduced to CdS films by sulphur evaporation may also account for the film's poor electrical characteristics, which are shown at higher temperatures.

$(Cu_{1-x}Ag_x)_2ZnSnS_4$ (CAZTS) thin films have been prepared by thermal evaporation [15]. The energy bandgap is an essential metric for solar cell applications since it establishes the wavelength of light that a material can absorb. With an increase in Ag concentration, the energy bandgap was observed to fall from 1.74 eV to 1.55 eV. The main photovoltaic properties of the n-CdS/p-CAZTS junctions were described, and the ITO/n-CdS/p-CAZTS/Mo heterojunction was expertly created. The presence of silver will absorb light, and the resonance effect can increase light trapping inside semiconductor layers by lengthening photons' paths through the material. Increased light absorption leads to an increased rate of electron-hole pair formation, which is essential for improving the photocurrent and overall efficiency of the cell. The Ag-based doping procedure may potentially impact the films' crystalline structure. Ag inclusion can improve semiconductor quality by perhaps generating a more ordered crystalline lattice that would otherwise serve as recombination centers. Reduced recombination sites increase the likelihood that charge carriers will reach the electrodes before recombining, hence extending carrier lifetime and improving device efficiency. The performance of the solar cells was enhanced by adding silver (Ag) to the $(Cu_{1-x}Ag_x)_2ZnSnS_4$ films (Ag from 0 to 0.5). This was because silver has a better electrical conductivity than copper (Cu). Ag can be used in place of Cu in the kesterite structure to increase the material's overall electrical conductivity. Better charge carrier movement inside the semiconductor may be made possible by this increase in conductivity. Second, the films' I_{sc} and V_{oc} improved when the Ag concentration was raised from 0 to 0.5. Since they have a direct impact on the solar cell's total efficiency, these variations are usually observed. Third, considering elements like charge carrier mobility and recombination losses, the fill factor parameter shows how well the solar cell transforms incident light into energy. Silver may be added to increase the fill factor by increasing the mobility of the charge carrier. Fourth, the best indicator of a solar cell's ability to convert sunlight into energy is its power conversion efficiency. The total PCE of the solar cell may be raised by including Ag to improve the I_{sc}, V_{oc}, and fill factor.

Flexible CZTSSe solar cells have garnered a lot of interest because of their excellent stability, abundance of earthly components, and several potential applications. The sputtering method was used to manufacture ZnO thin film, in which the ZnO target was exposed to an RF power source. Photovoltaic properties [16] will be affected by annealing temperature (150 to 250 °C), as highlighted in Table 3. With a power conversion efficiency of 5%, V_{oc} of 301.3 mV, I_{sc} of 37.8 mA/cm^2, fill factor of 44.0%, and an annealing temperature of 200 °C, the greatest device performance (CZTSSe/ZnO solar cell) is attained.

However, when annealing at 250 °C, efficiency drops to 1.6%, but shunt conductance increases. The flexible device that was produced at 200 °C during the annealing process has the lowest values of series resistance (1.7 Ω·cm^2) and shunt conductance (8.4 mS/cm^2), along with a better diode ideality factor (2.4). On the other hand, the device's EQE dramatically decreases at 250 °C. This condition can damage the CZTSSe/ZnO heterojunction's structure, which raises interface recombination and reduces performance. A $(Ge_{0.42}Sn_{0.58})S$ thin film was created by co-evaporation technique [17]. The thin-film solar cells had an open circuit voltage of 0.29 V, a short circuit current density of 6.92 mA/cm^2, a fill factor of 0.34, and a power conversion efficiency of 0.67%, respectively. In addition, the device had a band gap of 1.42 eV–1.52 eV. The solar cell based on $(Ge_{0.42}Sn_{0.58})S$ thin films had a slightly lower short circuit current density than SnS thin films.

Table 3. Photovoltaic properties of films annealed at various temperatures [16]

Annealing temperature (°C)	V_{oc} (mV)	I_{sc} (mA/cm^2)	Fill factor (%)	Power Conversion Efficiency (%)
150	287	34.9	44.8	4.4
200	301.3	37.8	44	5
250	206.1	24.3	31.7	1.6

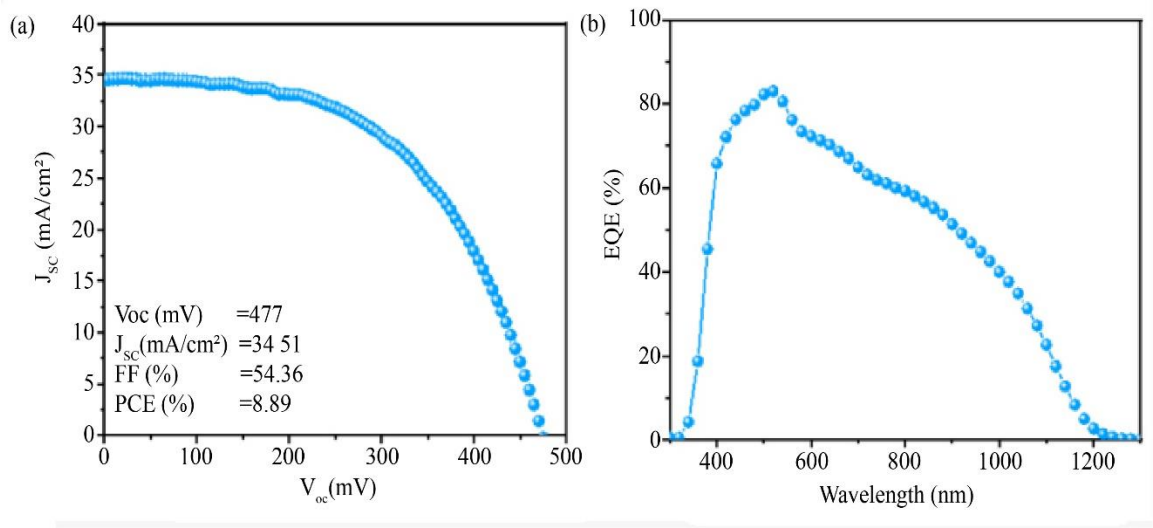

Fig. 1 J-V properties [a] and EQE response [b] of the CZTSSe films [18]

This could be due to different phases. Annealing reduced the film thickness while increasing the (Ge+Sn)/S composition ratio. However, the Ge/(Ge+Sn) composition ratio remained unchanged. This may be explained by sulfur re-evaporating during the annealing process. The grain appearance in SEM photographs is that of elongated platelets. It is believed that annealing caused the observed 1–5 µm grains, which are much bigger than those of SnS, to crystallize. The film was not preferentially orientated in one direction, according to the XRD data, but each grain's orientation was thought to be distinct since the film contains peaks that may be linked to (111) and (040). Additionally, they have shown that compared to a plane parallel to the substrate, a plane perpendicular to the substrate greatly enhances mobility in the thickness direction, making it a suitable configuration for solar cells.

In highly efficient CZTSSe devices, decision trees (DT) and classification and regression trees (CART) techniques provide the most appropriate composition windows for the device parameters. During the experiment, several artificial neural networks (ANN), XGBoost (XGB), SVM, and KNN algorithms demonstrated their applicability via prediction accuracy. The ideal composition ratios for the CZTSSe device [18] were Cu/Zn=1.15–1.20, Cu/Sn=1.25–1.30, Zn/Sn=0.95–1.0, and Cu/(Zn+Sn)=0.57–0.62. Crystalline thin films exhibiting distinctive CZTSSe peak at 2θ values of 27.27°, 45.31°, and 53.69° according to XRD studies. The production of big, compact grains (thickness of 1.65 µm) was revealed by the FESEM investigation. In terms of I_{SC}, V_{OC}, and fill factor, the device with an ML-optimized composition range demonstrated an average device power conversion efficiency of 8.61%, 33.61 mA/cm^2, 479 mV, and 53.51 %, correspondingly. The top devices measured external quantum efficiency (figure 1) and showed about 80 % photo response in the visible spectrum. Furthermore, an analogous device was projected to have bandgap values of 1.09 eV.

CuS thin films with a thickness of 500 nm were formed at ambient temperature over a soda-lime glass substrate coated with molybdenum [19]. Specifically, 60 W of RF power, 300 °C of substrate temperature, and 1.5X10^{-2} Torr (2 Pa) of working pressure were used to stack 500 nm thick SnS films on top of produced CuS thin film. CuS thin-film FESEM pictures show a smooth and uniform surface formed of relatively tiny dense particles with small void spacing under 40 W of RF power. Grain boundaries and size rose steadily when the deposition power was raised to 100 W. This result was consistent with the findings of the XRD study, which indicated that when the deposition power rose, the crystallite size improved, and the FWHM value reduced. The glass/Mo/absorber (CuS/SnS)/CdS/i-ZnO/ITO/Al solar cell with an active area of 0.4 cm^2 was reported to have a fabricated structure. When a CuS thin film was deposited at a power condition of 40 W, the solar cell's efficiency was 0.19%; for 60 and 80 W, the corresponding values were 0.25 % and 0.38 %, respectively (Table 4). The maximum efficiency of 0.39 % was observed at the 100 W power setting. With increasing power, the band-gap energy decreased, peaking at 2.57 eV for 60 W, 2.56 eV for 80 W, and 2.47 eV for 100 W. This is because the CuS thin film has thickened and improved in crystallinity. Sb_2Se_3 solar cells were created using the vapor transport deposition technique [20]. It is possible to regulate the growth rate and produce films that are pinhole-free, compact, conformal, and very thin.

Table 4. Photovoltaic characteristics of CuS/SnS absorber-based solar cells as a function of CuS sputtering powers [19].

Sputtering power (W)	Fill factor (%)	Power conversion efficiency (%)	I_{sc} (mA/cm^2)	V_{oc} (mV)
40	31	0.19	5.15	119
60	33	0.25	6.39	116
80	34	0.38	10.15	109
100	35	0.39	9.81	115

Furthermore, unlike the close-space sublimation technique, the high substrate temperature is unnecessary due to the reduced development rate and larger distance between the source and substrate. An optimized three-step deposition process may be used to build solar cells as thin as 0.4 µm Sb_2Se_3, and the results show that a short-circuit current density of more than 30 mA/cm^2 was attained. This demonstrates Sb_2Se_3 film's high absorption coefficient and potential for use in ultra-thin solar cells. As absorber thickness increased, short-circuit current density did not increase, indicating a corresponding decline in collecting efficiency and low open-circuit voltage (290 and 300 mV) was noted. Modern Sb_2Se_3 solar cells have a VOC of over 400 mV. This is because the built-in voltage, which was found using C-V measurements, suggests that there may be a Fermi-level pinning at the Sb_2Se_3–TiO_2 interface.

The distinct quasi-one-dimensional crystal structure of Sb_2Se_3 is mostly composed of $(Sb_4Se_6)_n$ ribbons. Compared to across the ribbons, the carrier transport efficiency along the $(Sb_4Se_6)_n$ ribbons is substantially greater. Therefore, it was crucial to use the right manufacturing processes to accurately regulate the development orientation of the Sb_2Se_3 thin films and guarantee that their vertical conductivity was increased to optimize Sb_2Se_3 solar cells. The near space sublimation technique has created high-quality antimony selenide films [21]. The findings showed that the right deposition durations helped achieve the desired film results, such as uniform grain distribution, moderate grain size, and decreased defect density. These factors improved carrier transport efficiency and, as a result, the devices' photovoltaic performance. Shorter deposition periods in SEM tests might have resulted in more densely dispersed grains, implying higher nucleation rates. Grain size influences carrier recombination rates and light absorption efficiency.

The interaction between the Sb_2Se_3 grains and the substrate is improved by extending the deposition period to 60 s. Furthermore, a more consistent pattern of longitudinal expansion for the (Sb_4Se_6)n band is noted. The morphology of the Sb_2Se_3 films shows a characteristic of vertically orientated grain dispersion in samples produced for 70 seconds. This phenomenon may have resulted from an elongation of the evaporation period, which increased the chances for crystal development and improved the orderliness and crystallinity of the crystals. Because of the longer evaporation period, the deposition rate was more constant, giving vapor phase atoms and molecules more chances to locate the best locations for lattice inclusion. Regarding photovoltaic characteristics (Table 5), solar device (FTO/SnO_2/Sb_2Se_3/P_3HT/C) performance significantly improves interface matching at 60 s. The resulting grains help to reduce interfacial compounding and absorb transport losses, offering more stable conditions. These results imply that increasing the deposition time optimizes the films' crystallinity and grain size, leading to a stronger (hk1) preferred orientation. As a result, thin films that are deposited for 60 seconds have better qualities. Cadmium is extremely harmful and may lead to various health problems. Cadmium is recognized as a human carcinogen and has the potential to harm the cardiovascular, reproductive, renal and respiratory systems. Copper indium gallium selenide (CIGS) can potentially substitute cadmium telluride films in solar cells. Because CIGS films are much less toxic, the appropriate band gap value (band gap=1.5 eV) still achieves similar efficiency and performance across various applications.

Additionally, a distribution gradient for gallium (Ga) has been discovered, and $CIGS_2$ has been studied as a potential absorber for the tandem configuration's top cell. Cu-poor (sample S1) absorber's grain size was seen to be marginally smaller in SEM pictures [22] than Cu-rich (sample S3) absorbers. Conversely, the Cu-rich absorber had a thinner layer than the Cu-poor absorber. Grain development may be markedly enhanced, and the Cu-rich (samples S2 and S3) CIGS2-absorption layer can reduce the fine-grain layer. The solar cells' current density-voltage characteristics were studied in the presence of light, with AM1.5G and 1000 W/cm^2 applied. With a short-circuit current of 15.53 mA/cm^2, an open-circuit voltage of 590 mV, and a conversion efficiency of 3.212 % (Table 6), sample S2 demonstrated the maximum efficiency of the $CIGS_2$-layer solar cell.

This resulted in an absolute gain of 2.304% when compared to the S1 cell. The greater CGI-ratio solar cell produced a bigger short circuit current value despite improving the fill factor. The produced samples' EQE impact was investigated. Because of the absorption layer's poor transmittance, the average EQE value rose as the CGI-ratio increased when the visible wavelength range was discovered to be between 400 and 700 nm. This was explained by the light absorption effect, wherein the absorber structure adopted a $CIGS_2$ bandgap that was smaller (1.61 eV), preventing more light from entering the primary absorption layer.

The efficiency of power conversion will be heavily dependent on deposition methods. For instance, the solvent evaporates rapidly in the spin coating because of centrifugal forces, resulting in a thinner film. Introducing antisolvent droplets during the spinning process can enhance the film quality and boost the efficiency of the solar cells.

Table 5. Photovoltaic properties of Sb_2Se_3 films prepared under different deposition periods [21]

Photovoltaic properties				Deposition time (seconds)
V_{oc} (V)	I_{sc} (mA/cm^2)	Power conversion efficiency (%)	Fill factor (%)	
0.284	20.05	2.704	47.43	40
0.318	22.01	3.794	54.19	50
0.352	26.79	5.067	53.76	60
0.295	23.51	3.047	44	70

Table 6. Photovoltaic properties of the $CIGS_2$-layer solar cells [22]

Sample	V_{oc} (mV)	Fill factor (%)	Power conversion efficiency (%)	I_{sc} (mA/cm^2)
S1	480	21	0.908	8.98
S2	590	34.8	3.212	15.53
S3	230	44.4	1.899	18.07

Glancing angle deposition refers to the process of applying vapor flux at an angle onto the surface of a substrate. It can be used to enhance the performance of films by adjusting the band gap and absorption co-efficient. Conversely, the vacuum evaporation method is the optimal technique for depositing optoelectronic devices. This method can generate high-quality thin films while presenting environmental issues and being cost-effective. The advantageous features of the deposited layer created by vacuum evaporation-based deposition methods include high mobility of charge carriers and a low carrier recombination rate.

The dependability of thin films is uncertain when compared to the rise and manufacturing of affordable, competitive crystalline silicon solar panels. A significant challenge confronting thin film based solar cells has been their reduced efficiency compared to the crystalline silicon based solar cells. Nevertheless, researchers are continually working to improve the effectiveness of thin film technology by creating innovative materials and production methods. A recent report from the International Energy Agency indicates that 2027 solar installed power capacity will surpass coal's, making it the largest. Through extensive research and development in materials science, several new thin film solar technologies with significant potential have arisen, including perovskite solar cells, organic solar cells and quantum dot solar cells. Both chemical and vacuum-based deposition processes have been used to create thin films. Because prepared films have a suitable band gap, a high absorption coefficient, and a cheaper production cost, they may be used for solar cells. Photovoltaic metrics, including fill factor, power conversion efficiency, open circuit voltage, and short circuit current, will be described and shown in this study. The results of the experiments validated that the behaviors of the characteristics were highly dependent on the experiment's settings.

3. Conclusion

The development of thin films for solar cells has advanced significantly due to improved deposition techniques, material optimization, and structural engineering. This review highlights the essential role of both vacuum-based and chemical deposition methods in creating thin films with suitable band gaps, high absorption coefficients, and cost-effective manufacturing. The photovoltaic performance of these films, including power conversion efficiency, fill factor, open circuit voltage (Voc), and short circuit current (Isc), is greatly affected by the deposition conditions and post-processing treatments. Research on materials like CZTS, CdS/CdTe, Sb2Se3, and CIGS shows that optimizing annealing temperature, elemental composition, and doping can boost solar cell efficiency.

New methods, including machine learning for material optimization and gradient bandgap engineering, hold potential for further advancements. However, challenges remain, such as lower efficiency compared to crystalline silicon solar cells and environmental concerns related to materials like cadmium. Future research should aim to improve the stability and scalability of thin-film solar cells, explore new high-efficiency materials, and develop sustainable manufacturing processes. Continued innovation in thin-film technology is essential for advancing renewable energy and making solar power more accessible and affordable.

Funding Statement

The author was financially supported by INTI International University, Malaysia.

Acknowledgments

This research work was financially supported by INTI International University.

References

[1] Bingyuan Zhao, and Alexander Wei, "Radiation-Tolerant Thin-Film Reference Electrodes and Potentiometric Sensors," *Sensors and Actuators B: Chemical*, vol. 416, 2024. [CrossRef] [Google Scholar] [Publisher Link]

[2] Ghazi Aman Nowsherwan et al., "Numerical Optimization and Performance Evaluation of ZnPC:PC70BM Based Dye-Sensitized Solar Cell," *Scientific Reports*, vol. 13, no. 1, pp. 1-16, 2023. [CrossRef] [Google Scholar] [Publisher Link]

[3] Jiawei Gong et al., "Review on Dye-Sensitized Solar Cells (Dsscs): Advanced Techniques and Research Trends," *Renewable and Sustainable Energy Reviews*, vol. 68, no.1, pp. 234-246, 2017. [CrossRef] [Google Scholar] [Publisher Link]

[4] Rahul Vishwakarma, "Effect of Substrate Temperature on ZnS Films Prepared by Thermal Evaporation Technique," *Journal of Theoretical and Applied Physics*, vol. 9, pp. 185-192, 2015. [CrossRef] [Google Scholar] [Publisher Link]

[5] Sreedevi Gedi et al., "Studies on Chemical Bath Deposited SnS_2 Films for Cd-Free Thin Film Solar Cells," *Ceramics International*, vol. 43, no.4, pp. 3713-3719, 2017. [CrossRef] [Google Scholar] [Publisher Link]

[6] N. Naghavi et al., "High-Efficiency Copper Indium Gallium Diselenide (CIGS) Solar Cells with Indium Sulfide Buffer Layers Deposited by Atomic Layer Chemical Vapor Deposition (ALCVD)," *Progress in Photovoltaics: Research and Applications*, vol. 11, no. 7, pp. 437-443, 2003. [CrossRef] [Google Scholar] [Publisher Link]

[7] Ji Hye Kim et al., "Growth of $Sn(O,S)_2$ Buffer Layers and Its Application to $Cu(In,Ga)Se_2$ Solar Cells," *Current Applied Physics*, vol. 14, no. 12, pp. 1803-1808, 2014. [CrossRef] [Google Scholar] [Publisher Link]

[8] May Zin Toe et al., "Effect of Reduced Graphene Oxide on the Structural, Optical, and Power Conversion Efficiency of ZnO Thin Film-Based Dye-Sensitized Solar Cells," *Thin Solid Films*, vol. 803, 2024. [CrossRef] [Google Scholar] [Publisher Link]

[9] Hechao Li et al., "Enhanced Mechanical Endurance and Power Conversion Efficiency in Flexible Cu_2ZnSnS_4 Solar Cells using ZnO/Ag-Ag_2O/ZnO Film," *Journal of Alloys and Compounds*, vol. 995, 2024. [CrossRef] [Google Scholar] [Publisher Link]

[10] Wei Han et al., "Effect of Tensile Strain on the Electronic Structure, Optical Absorptivity, and Power Conversion Efficiency of the BC_6N/ZnO Van Der Waals Heterostructure," *Physica E: Low Dimensional Systems and Nanostructures*, vol. 158, 2024. [CrossRef] [Google Scholar] [Publisher Link]

[11] Nandhakumar Eswaramoorthy, and Kamatchi Rajaram, "1D Graphitic Carbon Nitride Additive Modified ZnO Electron Transport Layer for Planar Perovskite Solar Cells: 12.22 % Power Conversion Efficiency over 1 cm^2 Active Area," *Diamond and Related Materials*, vol. 136, 2023. [CrossRef] [Google Scholar] [Publisher Link]

[12] Meenakshi Sahu et al., "Fabrication of Cu_2ZnSnS_4 Light Absorber Using a Cost-Effective Mechanochemical Method for Photovoltaic Applications," *Materials*, vol. 15, no. 5, pp. 1-16, 2022. [CrossRef] [Google Scholar] [Publisher Link]

[13] J. A. Melchor-Robles et al., "Characterization of CdS/CdTe Ultrathin-Film Solar Cells with Different CdS Thin-Film Thicknesses Obtained by RF Sputtering," *Coatings*, vol. 14, no. 4, pp. 1-11, 2024. [CrossRef] [Google Scholar] [Publisher Link]

[14] Gayan K. L. Sankalpa et al., "Enhancement of Photo-Electrical Properties of CdS Thin Films: Effect of N_2 Purging and N_2 Annealing," *Electronic Materials*, vol. 5, no. 1, pp. 30-44, 2024. [CrossRef] [Google Scholar] [Publisher Link]

[15] A.M. Bakry et al., "Increasing the Photovoltaic Efficiency of Semiconductor $(Cu_{1-x}Ag_x)_2ZnSnS_4$ Thin Films through Ag Content Modification," *Journal of Composites Science*, vol. 8, no. 8, pp. 1-19, 2024. [CrossRef] [Google Scholar] [Publisher Link]

[16] Quanzhen Sun et al., "Efficient Environmentally Friendly Flexible CZTSSe/ZnO Solar Cells by Optimizing ZnO Buffer Layers," *Materials*, vol. 16, no. 7, pp. 1-11, 2023. [CrossRef] [Google Scholar] [Publisher Link]

[17] Daiki Motai, and Hideaki Araki, "Fabrication of $(Ge_{0.42}Sn_{0.58})$ S Thin Films via Co-Evaporation and Their Solar Cell Application," *Materials*, vol. 17, no. 3, pp. 1-10, 2024. [CrossRef] [Google Scholar] [Publisher Link]

[18] Vijay C. Karade et al., "Unraveling the Effect of Compositional Ratios on the Kesterite Thin-Film Solar Cells Using Machine Learning Techniques," *Crystals*, vol. 13, no. 11, pp. 1-10, 2023. [CrossRef] [Google Scholar] [Publisher Link]

[19] Donghyeok Shin et al., "Effect of RF Power on the Properties of Sputtered-CuS Thin Films for Photovoltaic Applications," *Energies*, vol. 13, no. 3, pp. 1-12, 2020. [CrossRef] [Google Scholar] [Publisher Link]

[20] Remigijus Juskenas et al., "Seed Layer Optimisation for Ultra-Thin Sb_2Se_3 Solar Cells on TiO_2 by Vapour Transport Deposition," *Materials*, vol. 15, no. 23, pp. 1-10, 2022. [CrossRef] [Google Scholar] [Publisher Link]

[21] Jie Zhang, and Shanze Li, "The Effect of Deposition Time Optimization on the Photovoltaic Performance of Sb_2Se_3 Thin-Film Solar Cells," *Energies*, vol. 17, no. 8, pp. 1-14, 2024. [CrossRef] [Google Scholar] [Publisher Link]

[22] Tzu-Chien Li et al., "Optoelectronic Effects of Copper–Indium–Gallium–Sulfur ($CIGS_2$)-Solar Cells Prepared by Three-Stage Co-Evaporation Process Technology," *Micromachines*, vol. 14, no. 9, pp. 1-11, 2023. [CrossRef] [Google Scholar] [Publisher Link]